Chemical Engineering Science 229 (2021) 116022

Contents lists available at ScienceDirect

Chemical Engineering Science

journal homepage: www.elsevier.com/locate/ces

Contact angle measurements on cyclopentane hydrates

Fanny Thomas [a], Didier Dalmazzone [b], Jeffrey F. Morris [a,*]

[a] Benjamin Levich Institute and Dept. of Chemical Engineering, City College of New York, United States
[b] Dept. of Chemistry and Chemical Engineering, ENSTA Paris, Institut Polytechnique de Paris, France

HIGHLIGHTS

- The wetting properties of cyclopentane hydrates are investigated.
- A new experimental method to create smooth flat hydrate surfaces is proposed.
- The obtained surface is suitable for contact angles measurements.
- The surface is fully wetted by water when the other phase is oil or cyclopentane.
- Finite contact angles are obtained for halogenated hydrocarbons droplets in brine.

ARTICLE INFO

Article history:
Received 23 December 2019
Received in revised form 4 June 2020
Accepted 8 August 2020
Available online 12 August 2020

Keywords:
Gas hydrate
Flow assurance
Wetting
Cyclopentane
Contact angle

ABSTRACT

The wetting characteristics of clathrate hydrates influence their behavior in flow assurance situations, but these properties are not well-characterized. In this work, a new experimental method is proposed for measuring the contact angle of various liquids on cyclopentane hydrate, a structure II clathrate hydrate that forms at atmospheric pressure. This method includes a protocol to obtain a smooth flat hydrate surface, followed by standard image-based contact angle measurements. The protocol involves a succession of flipping and resting steps of a solid block, initially ice, immersed in liquid cyclopentane and subject to temperature variations around water freezing point, in order to allow progressive transformation to cyclopentane hydrate. Contact angle measurements on the flat hydrate surface were conducted for two sets of systems. First, water drops immersed in cyclopentane or various oils were observed to fully wet the hydrate surface. This result agrees with the surface tension values estimated by Aman et al. (2013) for the cyclopentane/hydrate/water system. Second, the contact angle of halogenated organic (dichloromethane, dichloroethane, and chloroform) drops immersed in brine was measured on cyclopentane hydrate and ice. Both the hydrate and ice surfaces were found to be water-wetting. Finite contact angles in the range of $125 \leqslant \theta \leqslant 149^\circ$ were obtained on the hydrate substrate. The ice substrate however, was observed to be fully wetted by the aqueous phase. Using the measured contact angles and interfacial tension of the liquid pairs, the work of adhesion for the hydrate surface and each of the halogenated organics was determined, and is comparable to values found in the work of Asserson et al. (2009) on freon hydrates.

1. Introduction

Clathrate hydrates have long presented a major concern in the petroleum industry (Hammerschmidt, 1934; Sloan, 2010). Clathrate hydrates, also called gas hydrates, are crystalline compounds with a hydrogen-bonded structure that can enclathrate, or ‘cage,’ various organic molecules, such as methane, propane or cyclopentane, or other small molecules such as hydrogen. Natural gas hydrates form at low temperature and high pressure and are found to be stable above the ice melting point (Hammerschmidt, 1934). As these conditions are prevalent in subsea pipelines transporting natural gas or crude oil, it is critical to manage hydrate formation and accumulation to avoid excessive pressure drop or even blockage in pipelines.

Today the methods used to maintain flowable conditions, i.e. methods for flow assurance, apply both thermodynamic and kinetic approaches. However, injecting thermodynamic inhibitors such as methanol or glycol to shift the pressure and temperature conditions for hydrate formation requires large volumes, and thus is limited in terms of efficiency and economic feasibility (Lee and

---

* Corresponding author.

E-mail addresses: fthomas001@citymail.cuny.edu (F. Thomas), didier.dalmazzone@ensta-paris.fr (D. Dalmazzone), morris@ccny.cuny.edu (J.F. Morris).

https://doi.org/10.1016/j.ces.2020.116022

Englezos, 2005). Recently, new strategies have emerged that include the use of low dosage hydrate inhibitors such as anti-agglomerants or kinetic inhibitors. These have been shown to effectively prevent hydrate agglomeration into large aggregated clusters: by affecting the interfacial properties of the system, these additives facilitate the transportation of hydrates as a slurry (Lee and Englezos, 2005; Kelland, 2006). Knowledge of the wetting properties of hydrates is therefore critical to optimize the use of these methods.

Understanding the rheological properties of hydrate forming emulsions is also directly relevant to flow assurance, and these properties have been argued to depend on capillary forces. Previous work has shown that hydrate slurries exhibit shear thinning behavior in general, and that an important parameter affecting the mechanical properties of the slurry is the initial water fraction and its fractional conversion to hydrate (McCulfor et al., 2011; Zylyftari et al., 2014; Zylyftari et al., 2015; Karanjkar et al., 2016). Zylyftari et al. (2013) studied the viscosity of a hydrate forming emulsion as a function of the maximum achievable water to hydrate conversion, at different shear rates and temperatures, with cyclopentane as the hydrate forming compound. This work reported a peak in viscosity at $61\% - 85\%$ conversion of water to hydrate, followed by a significant decrease as the water was fully converted to form a hydrate-in-oil suspension. It has been proposed that this behavior is related to the influence of forces acting between the hydrate particles due to capillary bridging between the particles (Aman et al., 2011; Yang et al., 2004; Karanjkar et al., 2016); in this case, the bridges are assumed to be formed of water since oil is the continuous phase. As can be seen in Fig. 1, the maximum in viscosity is attributable to the unconverted water of the system keeping the particles agglomerated in a connected network. As the water to hydrate conversion approaches 100%, there is decreasing influence of these cohesive forces between the particles arising due to capillarity, and the material reaches a lower viscosity. The interparticle forces due to capillary bridging strongly depend on the wetting conditions of the hydrate surface.

From the foregoing, it is clear that knowledge of the wetting properties of hydrates is an issue of primary importance in flow assurance. Determining the surface energy and related properties of hydrates provides critical input to efforts to improve our understanding of gas hydrate slurry structure and properties, and ultimately to support the goal of rationally designing methods to prevent agglomeration and plugging in pipelines. The wetting properties of a solid can be studied by measuring the contact angle of a liquid droplet sitting on a smooth and rigid surface (Drummond and Israelachvili, 2002; Israelachvili, 2011). However, hydrate nucleation and growth are stochastic in nature and obtaining a smooth and rigid hydrate surface is a challenging task. As a consequence, direct experimental measurements of the wetting properties of hydrate surfaces are not prevalent in the literature. Asserson et al. (2009) studied the wetting properties of freon (tradename by Chemours, CCl_3F [R11]) hydrate and the effects of various additives on the interfacial energy. These authors developed a method to create a smooth freon hydrate surface at the oil/water interface and measured contact angles of various hydrocarbon droplets sitting on this surface when it was immersed in the aqueous phase. Brown et al. (2018) reported finite contact angles for water droplets resting on cyclopentane hydrate particles with liquid cyclopentane as the surrounding phase, and provided estimates of the interparticle cohesion force. Surprisingly, this work reported a 94° contact angle, indicating that the hydrate surface is oil-wet and not water-wet as would be expected from a compound which is largely water and very similar to ice in structure. This counter-intuitive result, as well as a general lack of direct contact angle measurements on gas hydrate surfaces, further motivates our study. In this work, we develop a novel and robust method to create smooth, flat and rigid cyclopentane (CP) hydrate surfaces. We then report two sets of contact angle measurements: first, water drops immersed in cyclopentane or various oils on CP hydrate surface, and second, drops of halogenated organic compounds immersed in brine on both CP hydrate and ice surfaces.

2. Materials and methods

Materials For the hydrate-forming experiments, the oil phase was composed of liquid cyclopentane (98+% pure, Sigma Aldrich). Deionized water obtained from a Millipore QTM system was used as the aqueous phase. Cyclopentane (CP) is known to form structure II clathrate hydrates stable at atmospheric pressure with an equilibrium temperature of $T = 7.1$ °C (Sloan and Koh, 2007); this

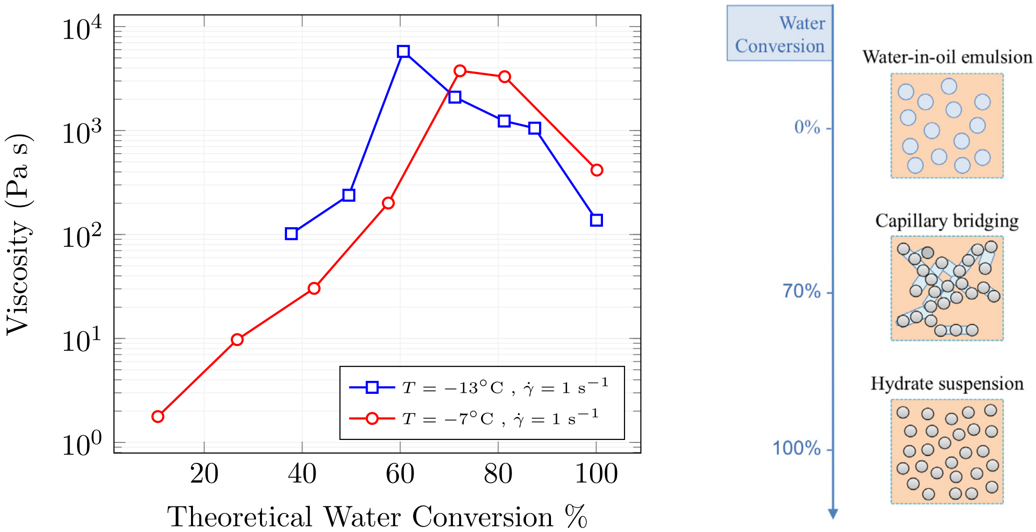
(a) Adapted from Zylyftari et al. (2013)

(b)

Fig. 1. Hydrate-forming emulsion (a) viscosity plot (adapted from Zylyftari et al. (2013)) and (b) postulated conceptual structure of the mixture as a function of theoretical water to hydrate conversion. The data are taken for $T < 0$ °C and at a shear rate of $\dot{\gamma} = 1$ s^{-1}. At 70% conversion the viscosity reaches a maximum because of capillary bridging between the newly formed hydrate particles. The cohesive forces due to the network structure depend on the wetting properties of the hydrate surfaces.

is a first-order phase transition rather than a reaction, and nucleation is stochastic and difficult to achieve without a template, so we form hydrate from melting ice as described in prior work (Zylyftari et al., 2014) and detailed for our conditions below. The stoichiometric ratio in CP hydrate is 17 molecules of water for one molecule of CP. Various liquids were used for the contact angle measurements; brine was obtained by dissolving 5% (w/w) sodium chloride (NaCl, hereafter simply salt) in deionized water. Several oils were tested against brine or water on the hydrate surfaces, and three chlorinated hydrocarbons were studied: dichoromethane, 1,2-dichloroethane and chloroform. Relevant physical properties of the materials used in this study are shown in Table 1.

As shown on Fig. 2, the samples were prepared in a cuvette of inner dimensions $20 \times 20 \times 24$ mm ($W \times L \times H$) and placed on a Peltier stage in a temperature controlled chamber for temperature variations between -30 °C and 90 °C. A thermocouple was introduced in the cuvette during the experiment to monitor the temperature and insulated windows on each side of the chamber allowed visualization of the hydrate formation and measurement of the contact angle.

Drop shape analyzer The temperature controlled chamber was mounted on a drop shape analyzer (KRUSS DSA25); images were captured using a high resolution camera equipped with a 6.5× manual zoom. The system was illuminated through the hatches of the chamber using a high power monochromatic light-emitting diode. The placement of the droplets and the position of the syringes was software-controlled and the real-time images were displayed and processed at the same time by the software (KRUSS ADVANCE). Interfacial tension between the droplet phase and the surrounding phase was measured using the pendant drop method (Stauffer, 1965). The shape of the drop, which results from the balance between interfacial tension and gravity, is analyzed by the software. The Young–Laplace equation,

$$\Delta P = \gamma\left(\frac{1}{R_1} + \frac{1}{R_2}\right), \tag{1}$$

is applied to shape to compute the value of interfacial tension between the two liquids. Here ΔP is the Laplace pressure and R_1 and R_2 are the principal radii of curvature.

Table 1
Materials physical properties.

Material	Chemical formula	Density at 20 °C (g mol^{-1})	Freezing point (°C)
DI Water	H_2O	1.00	0
Brine	H_2O + NaCl	1.02	−4.5
Cyclopentane	C_5H_{10}	0.75	−93.9
Dichloromethane	CH_2Cl_2	1.30	−96.7
1,2-Dichlorethane	$C_2H_4Cl_2$	1.20	−97
Chloroform	$CHCl_3$	1.50	−63.5

Theory and analysis of the surface properties The wetting properties of a solid surface can be characterized by measuring the contact angle of a sessile drop sitting on the surface at thermodynamic equilibrium. In particular, the balance of forces at the contact line, where the liquid/liquid interface meets the solid, yields Young's law (Young, 1805):

$$\gamma_{12} \cos\theta = \gamma_{2S} - \gamma_{1S}, \tag{2}$$

where γ_{12} is the interfacial tension between the two liquids, θ is the equilibrium contact angle, and γ_{1S} and γ_{2S} are the surface tensions between the solid and each of the liquids. By measuring θ and γ_{12} in our experiments, we can compute the difference $\gamma_{2S} - \gamma_{1S}$ and gain information on the surface properties of cyclopentane hydrate. Note, however, that $\gamma_{i,S}$ cannot be obtained separately. Another useful quantity is the work of adhesion of the liquid drop to the substrate, W_{12S}, defined as the energy per unit area needed to separate the droplet phase from the solid phase; this process removes the droplet/solid interface while creating two new interfaces, one between the surrounding phase and the droplet, and the other between the surrounding phase and the solid. The quantity W_{12S} can be calculated from the contact angle and interfacial tension values using the Dupré equation (Dupré and Dupré, 1869), which yields the Young-Dupré equation when combined with Eq. (2):

$$W_{12S} = \gamma_{12} + \gamma_{2S} - \gamma_{1S} = \gamma_{12}(1 + \cos\theta). \tag{3}$$

It should be noted that Eqs. (2) and (3) are only valid for an ideal surface. For surfaces that are not perfectly smooth, flat and chemically homogeneous, the equilibrium contact angle is not unique and depends on whether the liquid is advancing or receding on the surface (De Gennes, 1985; Israelachvili, 2011). Consequently for those surfaces, the work of adhesion varies locally as the droplet has to overcome local energy barriers to wet the surface. To account for the contact angle hysteresis produced by surface roughness and/or chemical heterogeneity in this work, each experiment was repeated over a large number of droplets deposited at different locations on the hydrate surface, and for multiple replicates of the same material. The contact angles were measured over time for chemically stable systems (that is, no further hydrate formation is expected). The results reported in the next section are the average values calculated from all the measurements for each system.

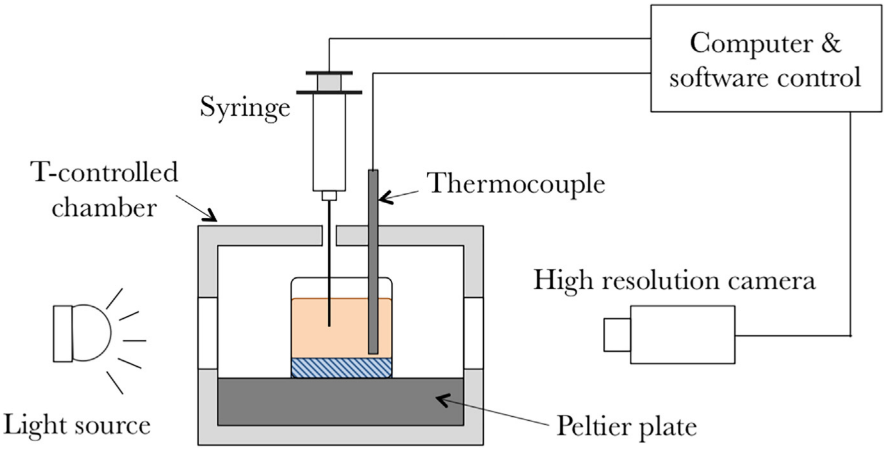

Fig. 2. Schematic of the experimental setup.

3. Results and discussion

3.1. Experimental procedure: formation of a flat hydrate surface

Hydrate formation consists of two steps: nucleation and growth. Previous work has shown that nucleation occurs at the oil–water interface and that for cyclopentane hydrates, growth will also be limited to that liquid/liquid interface in absence of any surfactant (Karanjkar et al., 2012; Zylyftari et al., 2013), but this surface is generally not smooth. This generates the challenge for wetting studies. To enable droplet deposition and measurement of meaningful contact angles, the hydrate surface needs to be as smooth as possible. Developing a robust and reproducible method involves finding the balance between a systematic nucleation and a controlled and slow growth of the hydrate layer.

Method development In the exploratory phase, deionized water and cyclopentane were layered in the cuvette in stochiometric proportions, forming an interface at the center of the cuvette. The sample was left at rest in the chamber overnight at constant temperature $T < T_{eq}$. Spontaneous nucleation, however, is very improbable at low subcooling temperatures (Mullin, 2001; Sloan and Koh, 2007). Classical methods to initiate nucleation such as stirring or hydrate seeding led to a quick growth of the hydrate layer, but with a resulting structure not suitable for droplet deposition.

Another means of starting the nucleation is to seed the solution with ice; in particular, it was shown that the water to hydrate conversion rate is qualitatively controlled by the temperature ramp of the experiment (Zylyftari et al., 2014), i.e. the ice melting rate. Ice seeding was also observed to be less effective than hydrate seeding, which in the context of our study is an advantage for a more controlled growth at the interface. To test this method, the temperature in the chamber was first lowered to $-20\,^\circ\mathrm{C}$ to freeze the water layer, then slowly raised above the melting point of ice but below the hydrate equilibrium temperature. Several temperature ramps were tested. The hydrate layer was then left to grow at rest in the chamber. With this method, similar to the one used by Brown et al. (2018), a uniform coverage of the interface by hydrate could be observed, with no pores visible at the macroscopic scale. As seen in Fig. 3a, the surface obtained with this method was rigid

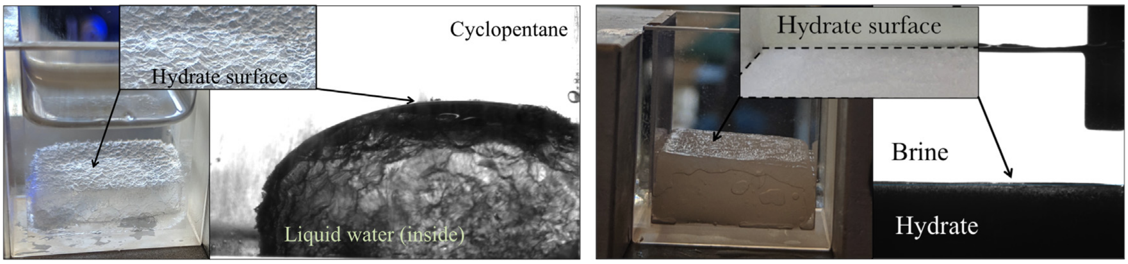

(a) (b)

Fig. 3. Formation of a flat hydrate surface. (a) Preliminary method yields a uniform but non-smooth coverage of the interface by the hydrates. (b) With the proposed protocol, a smooth and rigid surface is obtained. Comparison of the inset images illustrates the improvement in smoothness.

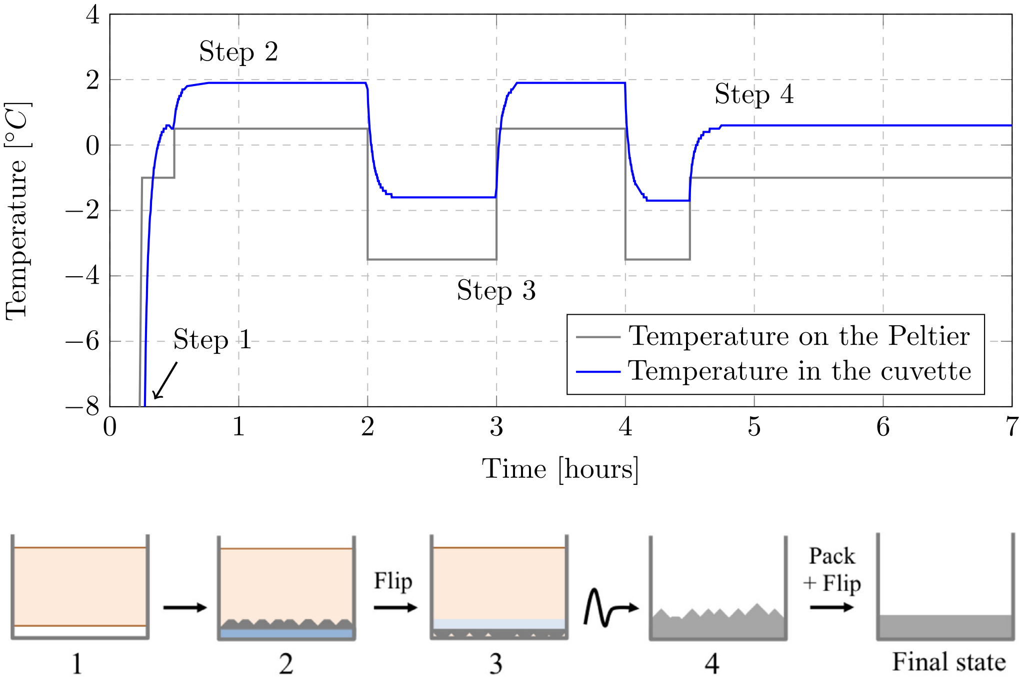

Fig. 4. Experimental procedure for the formation of a flat hydrate surface. The sample is submitted to temperature variations around water freezing point and manually flipped between steps to induce hydrate nucleation at the interface and water-to-hydrate conversion on each side. The offset between the temperature set on the Peltier plate and the actual temperature in the cuvette at the CP/water interface is due to the temperature gradient in the chamber and was continuously measured with a thermocouple during the experiment.

enough for a droplet to be deposited on the cyclopentane side, but exhibited a somewhat rough or 'spiky' structure. This surface roughness may induce droplet pinning and make the contact angle measurements inaccurate. Therefore another procedure, also using seeding by ice, was developed to improve the smoothness of the hydrate surface.

Final protocol A thin layer of deionized water (volume about 0.5 mL) was immersed in liquid cyclopentane and submitted to temperature variations around the freezing point of water, i.e., 0 °C, allowing for successive nucleation events and slow conversion to hydrate. The procedure to obtain the flat hydrate surface is illustrated schematically in Fig. 4 and follows the steps below:

1. Temperature T was lowered to $-20\ ^{\circ}\mathrm{C}$, inducing ice crystallization of the water layer immersed in cyclopentane.
2. T was slowly raised above ice melting point and held constant at $T = 0.5\ ^{\circ}\mathrm{C}$, initiating hydrate nucleation at the CP-water interface.
3. Temperature was lowered to $T = -3.5\ ^{\circ}\mathrm{C}$ to freeze the underlying water layer and the solid sample was manually flipped in the liquid CP by sliding a scalpel against the side wall of the cuvette. The hydrate layer was now lying against the bottom wall of the cuvette.
4. The temperature was raised once again above the ice melting point to initiate nucleation at the new CP-water interface. A last temperature cycle around the melting point promoted conversion of the remaining water into hydrate, and the sample was left overnight at $T = +0.5\ ^{\circ}\mathrm{C}$.

Table 2
Selected liquid–liquid systems for contact angle measurements.

System	Surrounding phase	Drop phase
1	cyclopentane	DI water
2	oils (pump, silicone, olive and canola)	brine
3	brine	dichloromethane
4	brine	1,2-dichlorethane
5	brine	chloroform

After the overnight rest period, the cyclopentane had evaporated and a solid hydrate sample was left in the cuvette. It was packed to form a flat rectangular block and flipped one last time. The side that was lying against the bottom wall before flipping is a flat, smooth and rigid cyclopentane hydrate surface. The sample obtained with this method was left in the chamber at $T = 2\ ^{\circ}\mathrm{C}$ for several hours to ensure that there was no residual ice (no melting) and to allow for evaporation of any residual cyclopentane.

3.2. Wetting properties of cyclopentane hydrates

The hydrate surface is maintained at the bottom of the cuvette using a pin and immersed in the surrounding phase. A droplet of a denser liquid immiscible with the surrounding phase is then deposited on the surface. Images of the spreading dynamics of the droplet are recorded and the equilibrium contact angle in the case of partial wetting is measured. All the systems tested in these experiments are summarized in Table 2. Each system includes an aqueous phase (pure deionized water or brine) and an oil- or hydrocarbon-based phase. The cell in which the measurements are conducted is partly isolated from the atmosphere of the lab. Therefore, it is expected to be near saturation in the organic surrounding phase vapour (brine/water or cyclopentane) at the operation temperature.

Set 1: Water droplet immersed in oil or cyclopentane In systems 1 and 2, the hydrate surface was immersed in cyclopentane or one of various oils at $T = 1.5\ ^{\circ}\mathrm{C}$. A droplet of the aqueous phase (deionized water or brine in systems 1 and 2, respectively) was then deposited on the surface. In all of these cases, near total wetting of the surface by the droplet was observed. Fig. 5 shows the spreading dynamics of a 20 μL droplet of deionized water in cyclopentane on the hydrate surface. Within seconds of the deposition, the macroscopic contact angle decreases to less than 10°.

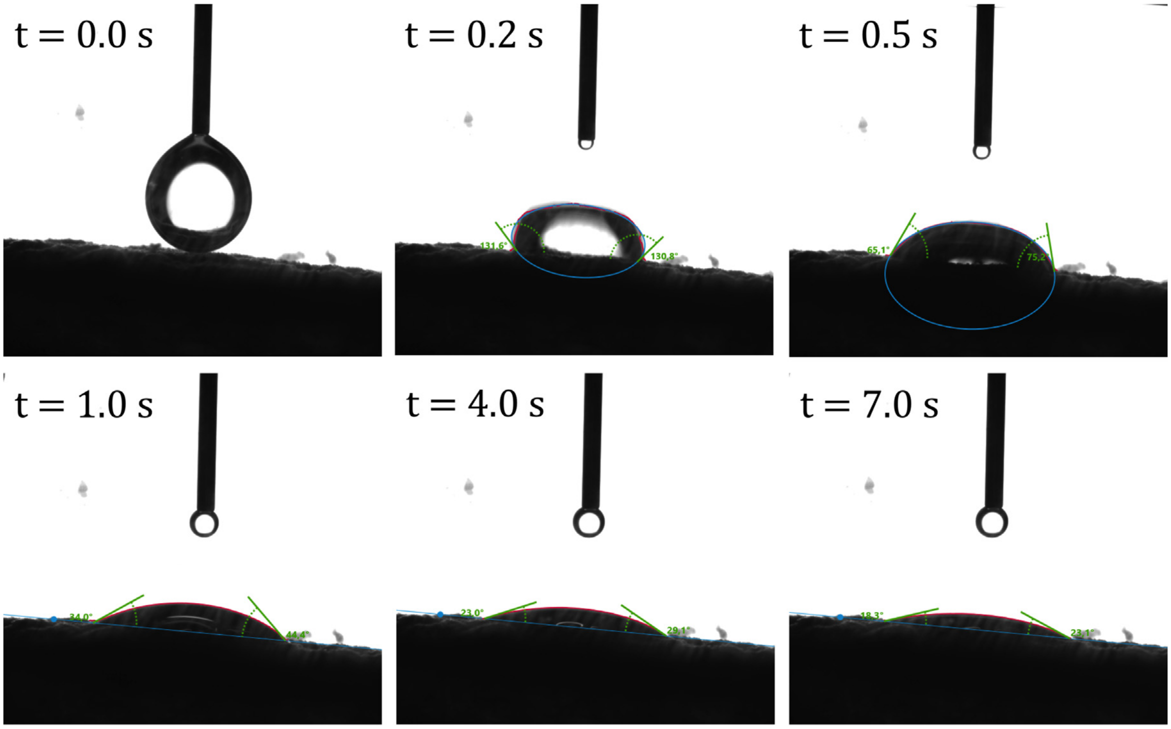

Fig. 5. Spreading dynamics of a water droplet on the hydrate surface. The system is immersed in cyclopentane. The hydrate surface is fully wetted by water. $T = 1.5\ ^{\circ}\mathrm{C}$.

Smaller contact angles could not be measured because new hydrates quickly started to form on the surface of the droplet after the first ten seconds. The experiment was repeated with multiple droplets and on the surface of separately formed hydrate samples, each formed by the same protocol. Even surfaces with visible asperities, including surfaces obtained with the preliminary method described in the previous section, did not prevent rapid spreading of the water droplet. The cyclopentane hydrate is highly water wet, as we would expect from a material composed largely of water and close to ice in structure. Aman et al. (2013) estimated the surface tension of hydrate/cyclopentane and hydrate/water at 47 ± 5 mN/m and 0.32 ± 0.05 mN/m, respectively, and a water/cyclopentane interfacial tension of 51 mN/m. Applying Young's law with these values yields a small equilibrium contact angle for a water droplet in cyclopentane sitting on the surface, which corroborates the assumption of a hydrophilic hydrate surface. Our findings do not, however, agree with the results obtained by Brown et al. (2018), who reported a water-in-cyclopentane contact angle of $94.2^\circ \pm 8.5^\circ$ on a CP hydrate particle. A contact angle of the water droplet greater than 90° means that the hydrate surface is hydrophobic, which would be very surprising. Indeed both the cage-like structure of gas hydrate compounds, which is made of water molecules, and the strong capillary forces involved in particle agglomeration and pipeline plugging, are consistent with water-wet rather than oil-wet surface properties. It is conjectured that in Brown et al. (2018), hydrate formation from the water of the spreading droplet occurred at the contact line soon after deposition and pinned the droplet on the surface, resulting in a misleading and unreliable measurement of the contact angle. Differences in temperature between the liquid phases may affect the spreading dynamics of the droplet: hydrate would more likely form at the contact line if the droplet is equilibrated in temperature with the surrounding phase. For system 1, the droplet was directly deposited on the substrate without being equilibrated beforehand. This might have allowed for a short time without pinning of the contact line and near full wetting of the surface by the slightly warmer droplet could be achieved, before new hydrates started to form.

The relevance of total removal of the hydrate-forming cyclopentane was confirmed by system 2. Total wetting of the hydrate surface by water was obtained for system 2 with any of the oils (pump oil, silicone or vegetable oil) as the surrounding phase. In this case, no residual cyclopentane was left in the cuvette, and the total spreading of the droplet could be recorded without any new hydrate nucleating on the surface as the hydrate former is absent. Within less than two seconds, the hydrate surface was fully wetted by the water drop, and no finite contact angle could be measured.

Set 2: Halogenated hydrocarbon droplet immersed in brine In systems 3, 4 and 5, brine (5% w/w) was the surrounding phase and a droplet of chlorinated hydrocarbon was deposited on the hydrate surface. The temperature in the system was about 1.5 °C. Brine was used instead of pure deionized water to avoid freezing for the experiments with ice as the substrate. For the ice systems, the temperature in the cuvette was kept constant at −2 °C.

The average contact angles obtained for each system and the standard deviation calculated from all the experiments are reported in Table 3. Example images captured and used for contact angle measurements are shown in Fig. 6. The contact angles measured are all higher than 90° which indicates that in all the systems, the hydrate surface is water-wet. The chloroform droplet forms the lowest contact angle, $\theta = 125^\circ \pm 1.4^\circ$, with dichloromethane forming the largest at $\theta = 149^\circ \pm 0.7^\circ$. These results are in general agreement with the range of values seen in the measurement of wetting by the same compounds on freon hydrate surfaces in the work of Asserson et al. (2009), although in that system, the smallest angle is seen for 1,2-dichloroethane. In all of these cases, the droplets are observed to rest steadily in contact with the substrate; no deterioration of the surface or pinning could be observed, and the contact angle measurements were stable over time. In addition to considering long-time measurement, in each case the average value presented is calculated from approximately 50 measurements; these are taken over multiple individual droplets, with measurement on each side of the droplet, and over separately formed hydrate sample surfaces, each formed following the same protocol.

Clathrate hydrates are often described as ice-like compounds because of their crystalline structure composed of water molecules forming hydrogen-bonded cages. Intuitively, we thus expect the wetting properties of hydrate and ice to be very similar, with a high affinity for water. For the three systems, however, the contact angles obtained with ice as the substrate differ measurably from those found with the hydrate substrate. As shown on Fig. 7, the droplets were not able to form a stable finite contact angle on the ice surface; dewetting of the droplet could be observed within the first seconds after deposition (as pictured on Fig. 7b), and the droplet would then roll off to the side wall of the cuvette if the ice surface was not sufficiently horizontal. The implication is that ice has a high affinity for brine in all systems and the hydrocarbon-substrate surface energy is lower for hydrate than for ice.

Table 3
Contact angles for the chlorinated hydrocarbons/brine systems

Droplet phase	θ at T=1.5 °C Hydrate substrate	θ at T=−1 °C Ice substrate	Asserson et al. (2009) Freon hydrate substrate
dichloromethane	$149^\circ \pm 0.7^\circ$	180° (dewetting)	$153^\circ \pm 2.9$
1,2-dichlorethane	$140^\circ \pm 3.4^\circ$	135°	$133^\circ \pm 5.1$
chloroform	$125^\circ \pm 1.8^\circ$	180° (dewetting)	$151^\circ \pm 5.7$

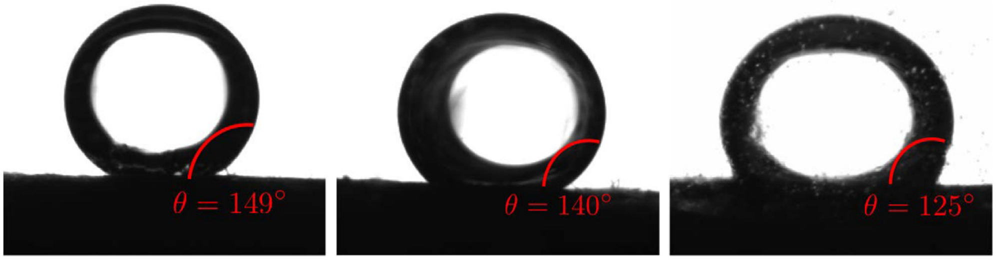

(a) Dichloromethane (b) 1,2-Dichloroethane (c) Chloroform

Fig. 6. Contact angles of various chlorinated hydrocarbon droplets sitting on the hydrate surface immersed in brine (5% (w/w)). $T = 1.5$ °C. The lowest contact angle was obtained with chloroform.

(a) Drops of halogenated hydrocarbons on ice vs. hydrate substrate

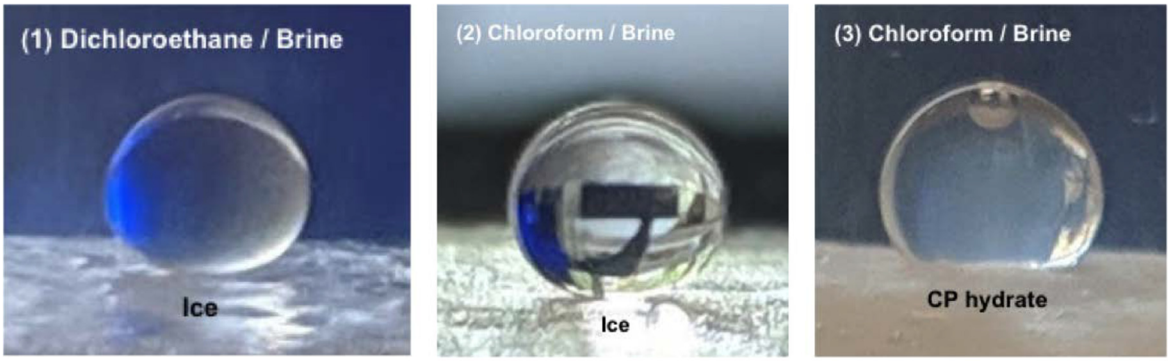

(b) Dewetting of a drop of dichloromethane on ice within seconds of deposition.

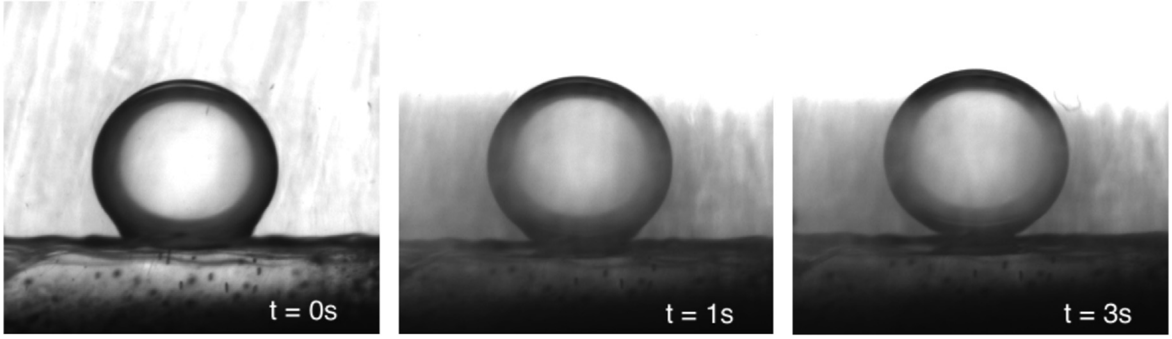

Fig. 7. The difference in the wetting properties of ice and cyclopentane hydrate surfaces. The surrounding phase is brine. (a) At equilibrium the hydrocarbon phase (dichlorethane or chloroform here) does not wet the ice ($\theta = 180^\circ$). The last picture (3) shows for comparison a drop of chloroform sitting on the hydrate surface with 125° contact angle. (b) The drop of dichloromethane instantaneously dewets the ice surface after deposition. Pictures taken at $t = 0, 1$ and 3 s, respectively, after droplet deposition. At $t = 3$ s, the contact angle is $\theta = 180^\circ$.

Table 4
Wetting properties of cyclopentane hydrates for the chlorinated hydrocarbons/brine systems at $T = 1.5\ ^\circ$C. Subscript 2 represents the surrounding phase (brine) and subscript 1 is the drop phase (hydrocarbon).

Droplet phase	Contact angle θ_e	Interfacial tension γ_{12} (mN/m)	Surface tension $\gamma_{2H} - \gamma_{1H}$ (mN/m)	Work of adhesion W_{12H} (mN/m)
dichloromethane	$149^\circ \pm 0.7^\circ$	27.9 ± 0.1	-23.9	4.0
1,2-dichlorethane	$140^\circ \pm 3.4^\circ$	26.5 ± 0.2	-20.3	6.2
chloroform	$125^\circ \pm 1.8^\circ$	27.7 ± 0.1	-15.9	11.2

Interfacial tension between the droplet phase and brine was measured using the pendant drop method at $T = 1.5\ ^\circ$C. Values are reported in Table 4. From Eqs. (2) and (3), the difference between the surface energies $\gamma_{2S} - \gamma_{1S}$ and the work of adhesion W_{12H} were computed. The interfacial tension values are similar for the three systems, as the chlorinated hydrocarbons have similar affinity for the aqueous phase. The difference $\gamma_{2S} - \gamma_{1S}$ is always negative, indicating that the drop phase is non-wetting for the hydrate surface, i.e. the hydrate surface is hydrophilic but not fully wetted by the water phase, unlike the systems 1 and 2 (see Table 2 for the system descriptions). The work of adhesion is the thermodynamic energy required to detach the droplets from the surface ($W_{12H} > 0$). This is found to be largest for chloroform, for which the work of adhesion on cyclopentane hydrate substrate is almost three times higher than that of dichloromethane on this surface. The surface tension γ_{1S} of chloroform against this hydrate is the lowest of all three systems, which means that the force exerted by the drop along the surface (towards the interior of the drop) is also the weakest. This agrees with the contact angle values only because the interfacial tensions γ_{12} are comparable for the three systems.

4. Conclusions

In this work, we have proposed a robust method to generate smooth, rigid and flat cyclopentane (CP) hydrate surfaces, with no pore or prominent asperity visible at macroscopic scale of the order of the mm drops. The hydrate surfaces obtained with this method were used for measuring the contact angle of various liquid droplets. The following results were obtained:

- The CP hydrate surface is fully wetted by water for the water-CP system and for the water–oil (silicone, pumping or vegetable) systems. The result for the water-CP system agrees with expectations and compares well with the surface tension values estimated by Aman et al. (2013).

- Finite contact angles, in the range of $125 \leqslant \theta \leqslant 149^\circ$, were obtained for various chlorinated hydrocarbon-brine systems on CP hydrate, indicating that the hydrate surface is hydrophilic, but not fully wetted by water. The values are in the same range as those obtained by Asserson et al. (2009) for these compounds on freon hydrates.
- The work of adhesion for each system was determined based on the interfacial tension and contact angle measurements, and estimated at $4.0, 6.2$ and 11.2 mN/m for the dichloromethane, 1,2-dichloroethane and chloroform drops in brine, respectively. We find that chloroform has the highest affinity for the hydrate surface.
- The wetting properties of CP hydrates differ from the ones of ice; none of the tested chlorinated hydrocarbon drops was able to wet the ice substrate immersed in brine (180° contact angle), showing that the hydrocarbon-substrate surface energy is lower for hydrate than for ice.

CRediT authorship contribution statement

Fanny Thomas: Formal analysis, Investigation, Validation, Writing - original draft. **Didier Dalmazzone:** Conceptualization, Funding acquisition, Methodology, Resources, Supervision, Writing - review & editing. **Jeffrey F. Morris:** Conceptualization, Data curation, Funding acquisition, Project administration, Supervision, Writing - review & editing.

Declaration of Competing Interest

The authors declare that they have no known competing financial interests or personal relationships that could have appeared to influence the work reported in this paper.

Acknowledgments

This material is based upon work supported by the National Science Foundation under Award Number 1743794. The Agence Nationale de la Recherche is also aknowledged for support of the MUSCOFI project under Award Number ANR-18-CE05-0028.

References

Aman, Z.M., Brown, E.P., Sloan, E.D., Sum, A.K., Koh, C.A., 2011. Interfacial mechanisms governing cyclopentane clathrate hydrate adhesion/cohesion. PCCP 13 (44), 19796–19806.
Aman, Z.M., Olcott, K., Pfeiffer, K., Sloan, E.D., Sum, A.K., Koh, C.A., 2013. Surfactant adsorption and interfacial tension investigations on cyclopentane hydrate. Langmuir 29 (8), 2676–2682.
Asserson, R.B., Hoffmann, A.C., Høiland, S., Asvik, K.M., 2009. Interfacial tension measurement of freon hydrates by droplet deposition and contact angle measurements. J. Petrol. Sci. Eng. 68 (3–4), 209–217.
Brown, E.P., Hu, S., Wells, J., Wang, X., Koh, C.A., 2018. Direct measurements of contact angles on cyclopentane hydrates. Energy & Fuels 32 (6), 6619–6626.
De Gennes, P.-G., 1985. Wetting: statics and dynamics. Rev. Modern Phys. 57 (3), 827.
Drummond, C., Israelachvili, J., 2002. Surface forces and wettability. J. Petrol. Sci. Eng. 33 (1–3), 123–133.
Dupré, A., Dupré, P., 1869. Théorie mécanique de la chaleur. Gauthier-Villars.
Hammerschmidt, E., 1934. Formation of gas hydrates in natural gas transmission lines. Ind. Eng. Chem. 26 (8), 851–855.
Israelachvili, J.N., 2011. Intermolecular and Surface Forces. Academic Press.
Karanjkar, P.U., Ahuja, A., Zylyftari, G., Lee, J.W., Morris, J.F., 2016. Rheology of cyclopentane hydrate slurry in a model oil-continuous emulsion. Rheol. Acta 55 (3), 235–243.
Karanjkar, P.U., Lee, J.W., Morris, J.F., 2012. Surfactant effects on hydrate crystallization at the water–oil interface: hollow-conical crystals. Crystal Growth Des. 12 (8), 3817–3824.
Kelland, M.A., 2006. History of the development of low dosage hydrate inhibitors. Energy Fuels 20 (3), 825–847.
Lee, J.D., Englezos, P., 2005. Enhancement of the performance of gas hydrate kinetic inhibitors with polyethylene oxide. Chem. Eng. Sci 60 (19), 5323–5330.
McCulfor, J., Himes, P., Anklam, M.R., 2011. The effects of capillary forces on the flow properties of glass particle suspensions in mineral oil. AIChE J. 57 (9), 2334–2340.
Mullin, J.W., 2001. Crystallization. Elsevier.
Sloan, E.D., 2010. Natural Gas Hydrates in Flow Assurance. Gulf Professional Publishing.
Sloan, E.D., Koh, C.A., 2007. Clathrate Hydrates of Natural Gases. CRC Press.
Stauffer, C.E., 1965. The measurement of surface tension by the pendant drop technique. J. Phys. Chem. 69 (6), 1933–1938.
Yang, S.-O., Kleehammer, D.M., Huo, Z., Sloan, E.D., Miller, K.T., 2004. Temperature dependence of particle–particle adherence forces in ice and clathrate hydrates. J. Colloid Interface Sci. 277 (2), 335–341.
Young, T., 1805. Iii. an essay on the cohesion of fluids. Philosoph. Trans. Roy. Soc. London 95, 65–87.
Zylyftari, G., Ahuja, A., Morris, J.F., 2014. Nucleation of cyclopentane hydrate by ice studied by morphology and rheology. Chem. Eng. Sci. 116, 497–507.
Zylyftari, G., Ahuja, A., Morris, J.F., 2015. Modeling oilfield emulsions: comparison of cyclopentane hydrate and ice. Energy Fuels 29 (10), 6286–6295.
Zylyftari, G., Lee, J.W., Morris, J.F., 2013. Salt effects on thermodynamic and rheological properties of hydrate forming emulsions. Chem. Eng. Sci. 95, 148–160.